Role of Auxiliary Gas Flow in Organic Sample Introduction With Inductively Coupled Plasma Atomic Emission Spectrometry

Changkang Pan,* Guangxuan Zhu and Richard F. Browner†
School of Chemistry and Biochemistry, Georgia Institute of Technology, Atlanta, GA 30332–0400, USA

Auxiliary gas flow exerts a much greater effect on plasma properties with organic sample introduction than with aqueous sample introduction. Changing the auxiliary gas flow rate causes a major shift in the distribution of solvent loading in the plasma sample injection channel, which in turn influences the plasma excitation conditions, causing changes in excitation temperatures and height-resolved emission profiles. Observations of plasmas run with xylenes, amyl alcohol and carbon tetrachloride show that C_2 emission signals are the clearest indicator of organic solvent–plasma interactions, changing significantly both with solvent type and with operating power. The CN band emission also varies as plasma conditions are changed, but C atomic emission is least sensitive to changes in plasma conditions.

Keywords: *Inductively coupled plasma atomic emission spectrometry; auxiliary gas flow rate; organic solvent; excitation temperature; sample introduction*

Solvent–plasma interactions play an extremely important role in determining analytical signal and background levels in inductively coupled plasma atomic emission spectrometry (ICP-AES). Although interactions of this type have received some study in recent years,[1–9] the focus in most investigations has been primarily from a perspective in which the influence of total solvent load on parameters such as plasma temperature and electron density has been examined. However, recent studies with aqueous sample introduction[1–3,10] have shown that in order to understand solvent–plasma interactions more deeply, it is necessary to examine them from the perspective of the unique environment surrounding an evaporating droplet in the plasma. By so doing, new mechanistic insights appear that have important implications for key ICP-AES performance parameters such as detection limits, precision and accuracy. For example, studies with aqueous solvents[3,10] have shown that the microscopic environment of a metal atom proceeding through a plasma is far more influenced by solvent evolving from a droplet than by the same solvent already present as vapour dispersed uniformly in the gas stream.

In general, organic solvents exert a much stronger influence than aqueous solvents on ICP properties.[4–13] Boorn and Browner[5] found that, in contrast to general experience with flame spectrometry, many organic solvents gave rise to strong signal suppressions, the magnitude of which were directly related to the volatility of the solvent. Signal suppressions arising from the use of organic solvents could generally be changed to signal enhancements by removing excess of solvent vapour with a condenser placed after the spray chamber, emphasizing the correlation between plasma excitation conditions and solvent interaction with the plasma. Boumans and Lux-Steiner,[6] studying isobutyl methyl ketone introduction, observed a net reduction of usable power in the plasma equivalent to approximately 500 W of applied r.f. power. Blades and Caughlin,[9] measuring plasma excitation temperatures and electron densities for xylenes introduction, also noted the same apparent equivalence of organic solvent loading and applied r.f. power. Confirming and broadening the conclusions of Boorn and Browner,[5] Kreuning and Maessen[12] observed that the chemical and physical nature of the solvents used were also highly important factors in determining plasma excitation conditions, and evolved the concept of a solvent load parameter as a means of characterizing the influence of difference solvents on the plasma.

There are basically three approaches suitable for studying mechanisms of solvent–plasma interactions. One option is to use the intensities of suitable emitting species, such as C, C_2, CN and OH, from the central plasma channel as diagnostic tools.[5,12] Organic solvents will give strong C_2 emission, whereas aqueous solvents will produce strong OH emission. With organic solvents, the degree of interaction of the solvent pyrolysis products with the plasma will depend substantially on the nature of the solvent. A second approach to studying solvent–plasma interactions is to monitor the total solvent loading on the plasma, and relate this to various plasma properties. Kreuning and Maessen[13] used this approach when measuring the excitation temperature profiles of an ICP as a function of organic solvent loading. Under these conditions they noted a direct correlation between increasing solvent loading and decreasing excitation temperature. In a previous study, the present workers[14] observed that the solvent mass transport rate for CCl_4 is ten times greater than that for water, which suggests that in this situation mass loading effects may overwhelm dissociation energy differences between C_2 and OH. Analyte and background emission spectra, emission height profiles and ion:atom intensity ratios were all found to be highly dependent on solvent loading on the plasma.[14]

A third approach to monitoring solvent–plasma interactions is to observe the distribution of solvent loading in the plasma central channel. Boorn *et al.*[4] observed that organic vapours may not pass entirely through the central channel of the ICP, but that a certain fraction of the vapour appears to pass around the base of the plasma. Only pyrolysis products of solvents present in the plasma central channel would be expected to exert a major influence on energy transfer into the plasma. From the perspective of the present study, it is important to note that the spatial distribution of pyrolysis products, such as C_2, in a central channel of the plasma may be altered by changing the auxiliary (intermediate) gas flow rate, without simultaneously changing the total solvent loading reaching the plasma or the nature of the pyrolysis products formed in the plasma.

The importance of the spatial distribution of organic solvent over the entrance paths to the plasma has been noted by previous workers.[4,13] From a practical perspective,[15] the use of auxiliary gas flow was found to enhance plasma stability by reducing carbon formation on torch

* Present address: Department of Chemistry, West Virginia University, Morgantown, WV 26506, USA.
† To whom correspondence should be addressed.

Table 1 Instrumentation and operating conditions

ICP	Plasma-Therm Model 1500
Torch	Fassel design
Nebulizer	Concentric type, Meinhard Model T-230-A3
Spray chamber	Glass cylinder, 20 cm × 3 cm i.d.
Forward power	1.5 kW
Reflected power	0–10 W
Argon flow rates:	
Plasma (outer)	14 l min^{-1}
Nebulizer (aerosol)	0.9 l min^{-1}
Liquid uptake rate	0.5 ml min^{-1}
Entrance slit	50 μm wide, 12.5 mm high
Mass flow controller	Matheson Model 8240
Pump	Buchler Multi-staltic pump
Data acquisition	Tracor Northern 1710
Detector	PDA TN-1223-21

surfaces. However, Boumans and Lux-Steiner[6] concluded that optimum signal-to-noise ratios were achieved with the lowest possible auxiliary gas flow rate. Consequently, although the practical importance of auxiliary gas flow rate for an organic plasma has been recognized for some time, very little is known at a fundamental level about the influence of auxiliary gas flow rate on plasma conditions.

This study was therefore directed towards the investigation and understanding of the effect of auxiliary gas flow rate on plasma basic properties. To this end, a comparison was made of organic and aqueous solvent introduction to an ICP under a wide variety of experimental conditions. Analyte emission spectra, emission–height profiles and ion:atom intensity ratios were measured as a function of auxiliary gas flow rate. As part of a diagnostic study of the plasma, emission characteristics of C, C_2 and CN species were also investigated at different incident r.f. powers.

Experimental

Instrumentation

A description of the instrumentation and operating conditions used in this study is given in Table 1. The plasma torch box was mounted on a counter-weighted platform, which could be positioned vertically with a resolution of 100 ± 10 μm. Radiation from the plasma source was focused on two orthogonal axes. On one of the axes a 0.35 m monochromator (GCA McPherson Model EV700) was mounted and adapted with a 512-element intensified linear photodiode array, which could be oriented vertically or horizontally in the exit focal plane. When the diode array was mounted vertically, emission intensity was measured as a function of height above the load coil and the emission height profile at one particular wavelength was obtained. The focused image of the plasma on the diode array was such that each array element viewed approximately 100 μm of the plasma vertically. When the photodiode array was mounted horizontally, the emission spectral window observed was approximately 50 nm. All emission–height profiles were background subtracted whereas the emission spectra were not.

Two separate spectrometric systems were used. In addition to the photodiode-array system described above, a 0.5 m Ebert scanning monochromator (Jarrell Ash Model 82-020) was used for spectroscopic temperature measurements. The spectrometer was equipped with a 1180 grooves mm^{-1} diffraction grating, providing a spectral resolution of 0.02 nm at an entrance slit setting of 25 μm × 2 mm. A Model R-106 photomultiplier tube (Hamamatsu TV) was used with a stabilized high-voltage power supply (6516A d.c., Hewlett-Packard) and a picoammeter (Keithley Model 414S). Readout was on to a strip-chart recorder (Fisher, Recordall Series 5000).

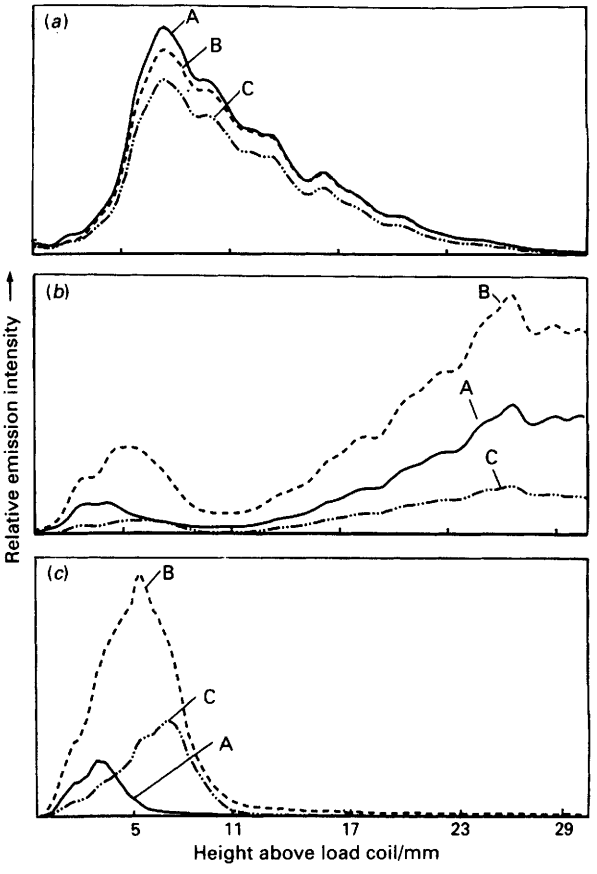

Fig. 1 Emission–height profiles for: (*a*) C (247.2 nm); (*b*) CN (358.5 nm); and (*c*) C_2 (512.0 nm). Solvents are A, amyl alcohol, B, CCl_4 and C, xylenes. Condenser temperature, −10 °C

Excitation Temperature

The Fe I lines used for temperature measurements were 371.993, 372.256, 372.762, 373.486 and 373.713 nm, with log *gf* values taken from Corliss and Bozman.[16] Measured line intensities were fitted with a least-squares routine using standard computer software. The values of log ($I\lambda^3/gf$) were plotted against excitation energy and excitation temperatures were calculated from the line slopes. The experimental standard deviation of the temperature was 40 K, based on ten repetitive measurements.

Reagents

Aqueous solutions were prepared by dilution of Fisher atomic absorption standards with de-ionized water (Continental water conditioning system). Organometallic standards (metal cyclohexanebutyrates; Eastman Kodak, standards for AAS) were used for the preparation of organic solutions. The dissolution procedure used was that developed previously in this laboratory.[5] For temperature measurements with water solvent, 250 ppm aqueous Fe solutions were used. For temperature measurements with CCl_4 solvent, 5000 ppm Fe solutions were prepared from ferrocene by first dissolving the solid in a minimum amount of xylenes (an unspecified mixture of *ortho-*, *meta-* and *para*-xylenes) and then diluting with CCl_4 to the desired concentration; CCl_4 and amyl alcohol were obtained from Fischer Scientific.

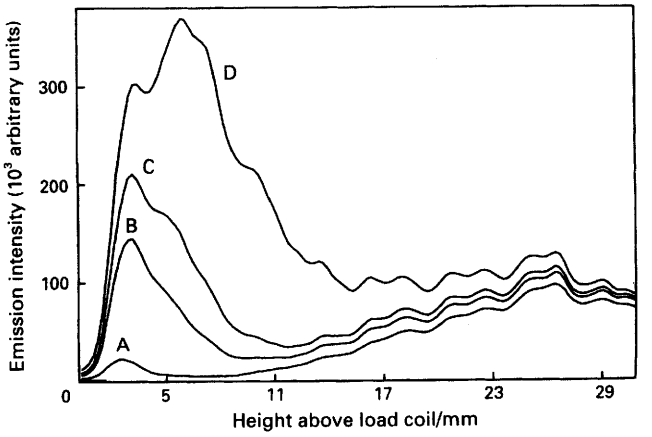

Fig. 2 Emission–height profiles for CN with nitrogen addition; nitrogen levels, A 0, B 1, C 2 and D 4%. Xylenes used as solvent with no condenser

Results and Discussion

Emission from Carbon Species in the Plasma

It has long been recognized[5,6,17] that organic solvents generate a variety of carbon species in the plasma. These are predominantly atomic carbon (C), diatomic carbon (C_2) and cyanide radical (CN). These species have distinctive emission characteristics, which can give rise to both spectral interferences and to degraded detection limits through a reduction in the signal-to-background ratio. It is very difficult to eliminate these species totally from plasma emission spectra, even by incorporating a low-temperature condenser in-line, although the plasma loading can be reduced considerably by this means. In this study, emission–height profiles were first measured at the major emission wavelengths of C, C_2 and CN (247.2, 512.0 and 358.5 nm, respectively) for three representative solvents (CCl_4, xylenes and amyl alcohol) and the results are shown in Fig. 1. It should be noted that the top of the plasma torch extended 3 mm above the load coil. Although some distortion of the image from the plasma must have occurred owing to a lens effect created by the cylindrical torch, this effect appears not to have been very significant. Observation of the vertical emission profiles showed no discontinuity occurring in any of them in the region corresponding to the top of the torch.

For this experiment only, a condenser run at −10 °C was placed after the spray chamber. For atomic C emission, the emission height profiles varied only slightly between the solvents. Maxima were all located approximately 8 mm above the load coil, and there were only small differences in peak intensities. For CN emission, two maxima were observed for all solvents, at viewing heights of approximately 5 and 25 mm, the major peak being at 25 mm. As suggested by Kreuning and Maessen,[13] the maximum at 25 mm is almost certainly the result of a reaction beween atomic carbon in the plasma and atmospheric nitrogen.

A subsidiary CN emission maximum was also observed approximately 5 mm above the load coil. Kreuning and Maessen[13] suggested that this subsidiary maximum results from nitrogen contamination in the argon gas. In order to test this hypothesis experimentally, a controlled flow of nitrogen was added directly to the spray chamber (the system was operated without a condenser in this instance), where it mixed with argon nebulizer gas, solvent vapour and solvent aerosol. The results are shown in Fig. 2. As expected, the subsidiary maximum, which is confined to the central plasma channel, was strongly dependent on the level of added nitrogen. Without nitrogen addition, the subsidiary maximum was very weak, but when the nitrogen level

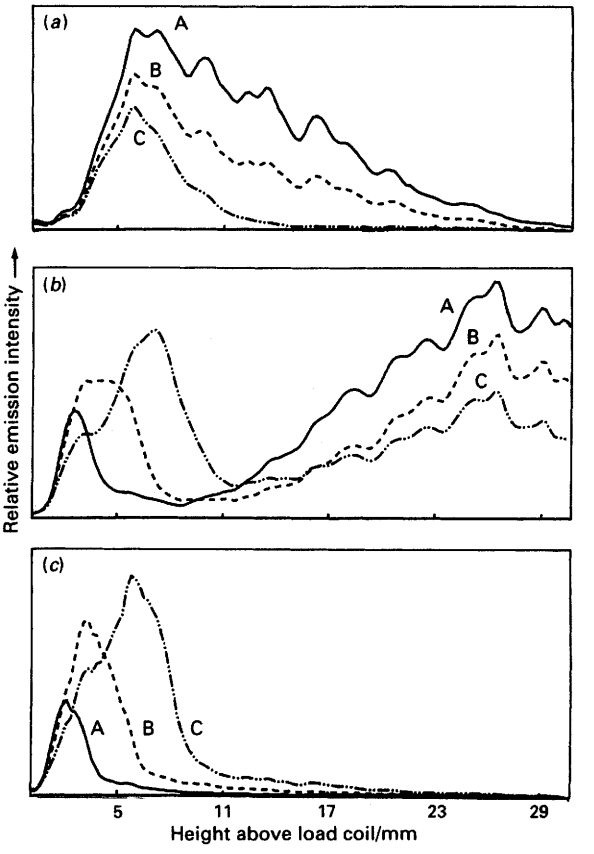

Fig. 3 Emission–height profiles of: (*a*) C (247.2 nm); (*b*) CN (385.5 nm); and (*c*) C_2 (512.0 nm) as a function of r.f. power. R.f. powers: A, 1000; B, 1250; and C, 1500 W. Solvent, xylenes

was increased from 1 to 4%, the CN emission intensity in the plasma central channel increased by a factor of 5. The increase in intensity was also accompanied by a shift in the position of the emission maximum from 2.5 to 6 mm. In contrast, the CN emission behaviour in the plasma tail was largely unaffected by nitrogen addition. In summary, both C atomic and CN emission signals are largely independent of the solvent, except for CN emission low in the plasma, which will be affected when either the solvent contains a nitrogen heteroatom or the argon is contaminated with nitrogen.

In contrast to C atomic and CN species, the C_2 emission–height profiles depend strongly on the nature of the solvent, and the positions of the peak maxima differ markedly with the nature of the solvent. Maxima were observed at 3 mm for amyl alcohol, at 5 mm for xylenes and at 7 mm for CCl_4. The visual appearance of the C_2 emission 'tongue' in the central aerosol channel is also noticeably different for different solvents.

Effects of R.f. Power on Carbon Emission Characteristics

It is often helpful to characterize line spatial profile behaviour in terms of the 'hard' and 'soft' nature of the lines.[18–21] Hard lines typically exhibit little spatial dependence on plasma power, whereas the emission maxima of soft lines generally shift lower in the plasma as the r.f. power is increased. Fig. 3 shows the emission–height profiles of C, C_2 and CN with xylenes solvent at three different r.f. power levels, from which the differences in their response characteristics are clear. For C_2 emission, an increase in power causes a large reduction in C_2 emission intensity, and at the same time shifts the peak maximum lower in the plasma. The C_2 maximum appears at 6 mm for 1000 W, at 3 mm for

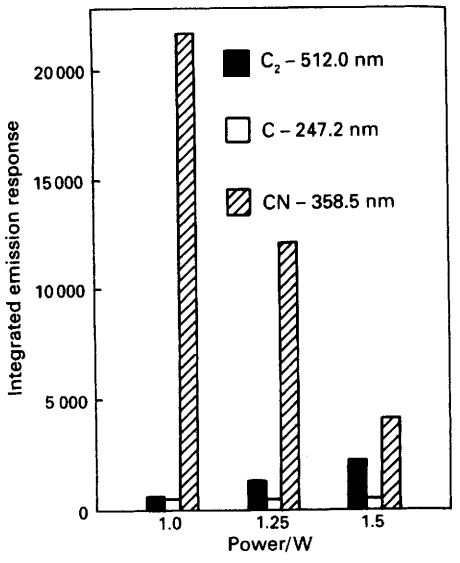

Fig. 4 Integrated background emission response for organic solvents as a function of r.f. power. Signal represents integrated area under the profile from 0 to 32 mm above the load coil. Solvent, xylenes

1250 W and at 2 mm for 1500 W. Consequently, C_2 emission at 512.0 nm exhibits apparent soft line behaviour, and both its intensity and maximum position vary inversely with r.f. power. This is readily explained in terms of energy transfer from the plasma to the C_2 species. Atomic C emission, in contrast, shows an apparent hard line response, with an increase in intensity with increasing r.f. power, and an approximately constant emission maximum 6 mm above the load coil. It should be noted, however, that signal enhancements were not symmetrical about the maximum with increasing r.f. power.

The CN emission exhibited some interesting features as a function of applied power, showing a noticeably different spatial dependence on power at different observation heights. In the plasma tail flame, CN emission behaves as an apparent hard line, with changes in plasma power causing little shift in the profile maximum, in a similar manner to C atomic emission. In the plasma central channel, however, CN emission behaves in the apparent manner of a soft line, and an increase in power from 1000 to 1500 W causes a distinct downward shift in the peak maximum by 4 mm. In the central channel, the availability of greater energy appears to favour the dissociation of CN species, resulting in a reduction of CN emission intensity and a downward shift in the profile. On the other hand, an increase in power also generates more excited atomic carbon species in the core of the plasma, which subsequently reacts with nitrogen to form a higher level of CN species high in the plasma, where there is inadequate power available to dissociate CN species totally.

The effect of power on the three carbon species is summarized in Fig. 4, where the data are expressed in terms of the integrated area under the entire emission height profile for each species, rather than the peak emission value at a selected height, in order to represent better the integrated excited state population in the plasma. The values are normalized to individual species emission magnitudes at 1000 W. The response functions for the three species are clearly different. An increase in r.f. power from 1000 to 1500 W causes the integrated emission for atomic C to increase threefold, C_2 emission to decrease fourfold and CN emission to remain almost unchanged. This does not imply that CN emission is unaffected by plasma power, only that local variations in CN emission are largely counterbalanced by compensating variations in CN emission at other observation heights. This is in general agreement with the observations of Barrett and Pruszkowska,[17] which were made at a fixed viewing height of 15 mm, monitoring atomic C, C_2 and CN emission intensities at 193.09, 436.52 and 359.04 nm, respectively. They concluded that an increase in r.f. power led to a rapid increase in C emission, a general reduction in C_2 emission and relatively little response change from CN emission. Overall, the influence of increasing power was considered to enhance the fragmentation of molecular species. However, observation at other measurement heights could lead to different conclusions. In the case of CN emission, for example, a measurement taken low in the plasma would show a reduction of CN emission with power, while an opposite conclusion would be drawn from observations made between 20 and 30 mm. At a viewing height of 15 mm, however, no net effect is observed. In this sense, detailed emission–height profiles provide a unique and helpful picture of species levels in the plasma.

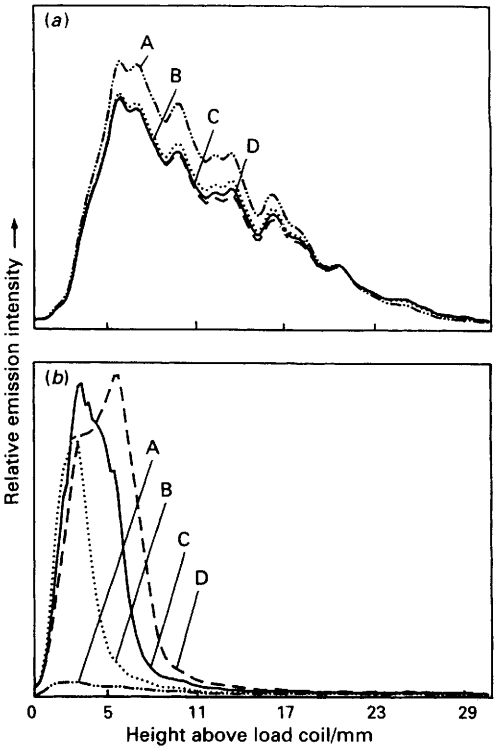

Fig. 5 Emission–height profiles of C (247.2 nm) and C_2 (512.0 nm) species at different auxiliary gas flow rates: A, 0; B, 0.9; C, 1.6; and D, 2.3 l min^{-1}. Solvent, xylenes

Effects of Auxiliary Flow Rate on Carbon Emission Patterns

The auxiliary gas influences gas and particle flow patterns in the vicinity of the base of the plasma, and therefore probably changes the extent of interaction of organic solvent vapour and aerosol with the plasma.[5] In this part of the study only the auxiliary flow rate was changed, all other parameters being held constant, so that the total solvent loading delivered to the plasma remained unchanged. Fig. 5 illustrates the C and C_2 emission height profiles obtained with xylenes at different auxiliary gas flow rates. The C emission profiles are seen to be insensitive to changes in auxiliary flow rate and the intensity maxima do not move. An increase in auxiliary gas flow rate from 0 to 0.9 l min^{-1} caused a reduction in C atomic emission intensity of only approximately 10%, with little change at higher flow rates. Additionally, no significant height–profile shift was ob-

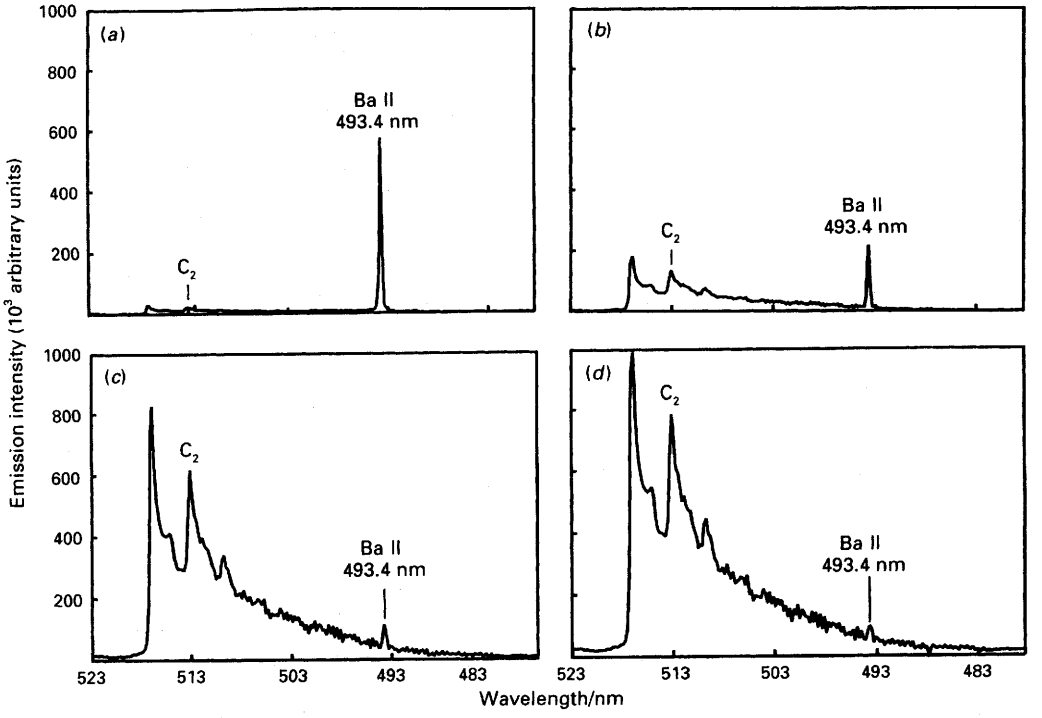

Fig. 6 Emission spectra of Ba II at (493.4 nm) at different auxiliary gas flow rates: (*a*) 0; (*b*) 0.9; (*c*) 1.6; and (*d*) 2.3 l min^{-1}. Observation height, 8 mm and solvent, CCl_4

served. In contrast, the effect on C_2 emission of increasing auxiliary flow rate was markedly different. In the absence of auxiliary gas, the C_2 emission intensity was minimal. As the auxiliary gas flow rate was increased, the C_2 emission intensity increased strongly and the height profile maximum also shifted higher in the plasma. The increase in C_2 emission is readily observed visually as a striking enhancement in the green C_2 'tongue' in the plasma.

A comparison of Figs. 3 and 5 suggests that an increase in auxiliary flow rate is basically equivalent to a reduction in applied r.f. power to the plasma. It therefore appears that a trade-off between these two factors should be possible, with changes in C_2 height profiles resulting from increased auxiliary flow rate being compensated for by an increase in plasma power. The most important function of the auxiliary gas appears to be to carry the sample more efficiently along the central flow axis of the sample injection stream, and hence to increase the analyte mass loading in the central channel of the discharge. However, changes in analyte aerosol transport are also accompanied by changes in solvent aerosol and solvent vapour transport to the plasma. As it is reasonable to assume that C_2 species are the dominant diatomic species present in the 'organic' plasma central channel, C_2 emission–height profiles can therefore act as a convenient diagnostic tool to monitor changes in the distribution of organic solvent loading in the plasma central channel, and to determine possible correlations with analyte excitation properties.

Effects of Auxiliary Gas Flow Rate on Atomic Line and Background Emission Features

The spectra shown in Fig. 6 illustrate the effect of auxiliary gas flow rate on the analyte and background emission for the 493.4 nm Ba II line. The spectra were taken at an observation height of 8 mm using CCl_4 as solvent. The broad band emission observed between 500 and 520 nm originates from C_2. It is apparent that in the absence of auxiliary gas, the C_2 emission background is weak and the barium ionic emission intensity is relatively strong. As the auxiliary gas flow rate is increased, the C_2 emission intensity increases and the Ba signal decreases. At a gas flow rate of 1.6 l min^{-1}, the organic plasma background is strong, and significant spectral overlap with the Ba II line occurs. Even more important, the net Ba ionic emission intensity is reduced by a factor of 8 as the auxiliary gas flow rate is increased from 0 to 1.6 l min^{-1}. Clearly, the signal-to-noise ratio for Ba determination deteriorates significantly at higher gas flow rates, and at a flow rate of 2.2 l min^{-1} the Ba emission signal became virtually undetectable. This agrees with the observations of Boumans and Lux-Steiner,[6] who found that the lowest possible auxiliary gas flow rates generally led to the best signal-to-noise ratios. However, with aqueous sample introduction, there was no noticeable differences in the background and analyte signals for Ba as the auxiliary gas flow rate changed. This emphasizes the solvent specificity of solvent–plasma interactions, and confirms the need to understand the role of gas and aerosol dynamics in order to predict and optimize analytical performance with different solvents.

Emission–height profiles for Ba 493.4 nm are shown in Fig. 7 as a function of auxiliary gas flow rate. The Ba emission profiles with aqueous solvent introduction do not appear to change much with auxiliary gas flow rate. As the gas flow rate is increased, the profiles low in the plasma shift only slightly higher. The emission maxima do not change noticeably, and the integrated area under the curve decreases only slightly. With CCl_4 solvent introduction, on the other hand, the emission profiles show a strong dependence on auxiliary gas flow rate. The Ba emission peaked at 15 mm with a flow rate of 0.3 l min^{-1}, but with a flow rate of 1.6 l min^{-1} the peak maximum shifted to approximately 20 mm above the load coil. This implies that an increase in the population of C_2 species in the sample injection channel results in a decrease in the effective plasma power low in the plasma, and so delays the onset of the analyte excitation process. Meanwhile, an increase in auxiliary gas flow rate causes dramatic decreases in the integrated areas under the emission profile curves, indicating that the populations of barium excited ionic species in the plasma are also reduced.

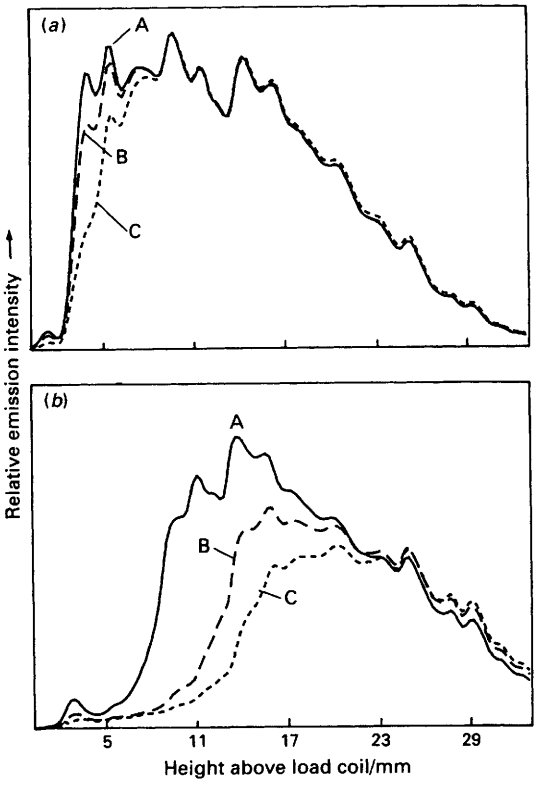

Fig. 7 Emission–height profiles of Ba II (493.4 nm) using (*a*) H_2O and (*b*) CCl_4 solvents at flow rates of: A, 0.3; B, 0.9; and C, 1.6 l min^{-1}

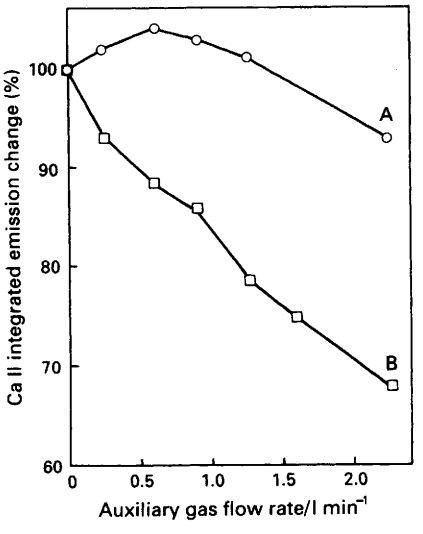

Fig. 8 Change in Ca II (393.4 nm) integrated emission intensity *versus* auxiliary gas flow rate: A, H_2O; and B, xylenes. Integration under profile from 0 to 32 mm above load coil

This behaviour is similar to that observed in an earlier study[14] in which solvent loading was changed by controlling the temperature of a condenser connected after the spray chamber. The similarity of behaviour suggests that for emitting species in the central channel of the plasma, increasing the auxiliary gas flow rate is comparable to increasing the solvent vapour loading in the plasma sample injection channel, although the total solvent delivery rate to the plasma remains unchanged.

The variation in Ca ionic emission is shown in Fig. 8 as a function of auxiliary gas flow rate for two different solvents. The Ca II 393.4 nm line, a typical hard line, was selected because it is free from spectral interference from C_2 emission in this wavelength region. The integrated emission area under the profile without auxiliary flow rate was selected as a reference, and the integrations at other flow rates were normalized to this value. It is clear that the effects of auxiliary gas flow rate on analyte signal depend strongly on the solvent used. With water as solvent, Ca II emission first increases with increasing flow rate, reaches a maximum at 0.6 l min^{-1} and decreases slightly at higher flow rates. However, the response change is only minor, with an optimum flow rate between 0.6 and 0.90 l min^{-1}.

With xylenes solvent introduction, however, the effect of auxiliary gas flow rate on the signal is different. An emission maximum was obtained only when no auxiliary gas was used, and an increase in auxiliary gas flow rate caused a continuous decrease in the emission signal. A net decrease in emission signal of 35% was observed as the auxiliary flow rate increased from 0 to 2.3 l min^{-1}. The lowest emission signal was obtained with the highest auxiliary gas flow rate.

Effects of Auxiliary Gas Flow Rate on Plasma Excitation Conditions

The importance of controlling the auxiliary gas flow rate may further be demonstrated by measuring ion-to-atom intensity ratios. The Mg II:Mg I ratio has long been used as a diagnostic tool for tracking plasma excitation and ionization conditions.[5,22] Fig. 9 shows how this ratio changes as a function of auxiliary gas flow rate for both organic and aqueous solvents. For an aqueous plasma, this intensity ratio shows little variation with changes in auxiliary gas flow rate. In an ICP with CCl_4 solvent introduction, however, a dramatic change is observed. The ratio is highest for the lowest gas flow rate, in this instance 0.3 l min^{-1}, and decreases by a factor of four as the flow rate is increased from 0.3 to 1.6 l min^{-1}.

The results mentioned above emphasize how much stronger the effect of auxiliary gas flow on plasma excitation conditions is in an 'organic' than in an 'aqueous' plasma. As further evidence for this point the variation in plasma excitation temperature as a function of auxiliary gas flow rate for aqueous and organic plasmas is contrasted in Fig. 10. Whereas the temperature shows little change with auxiliary gas flow rate for an aqueous plasma, when CCl_4 is introduced a considerable temperature drop is observed. When the auxiliary gas flow rate was increased from 0.3 to 2.3 l min^{-1}, the excitation temperature decreased by 500 K. As would be expected on the basis of C_2 emission behaviour, the greatest decrease in temperature was observed with the highest auxiliary gas flow rate.

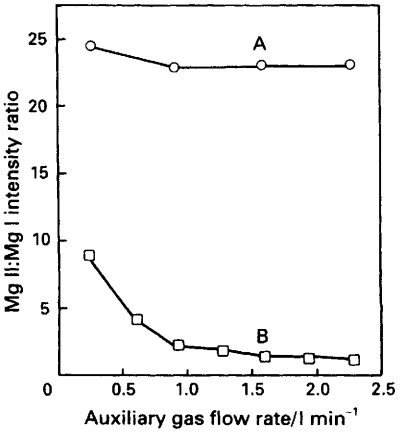

Fig. 9 Mg II:Mg I intensity ratio *versus* auxiliary gas flow rate: A, H_2O; and B, CCl_4. Observation height, 20 mm above the load coil

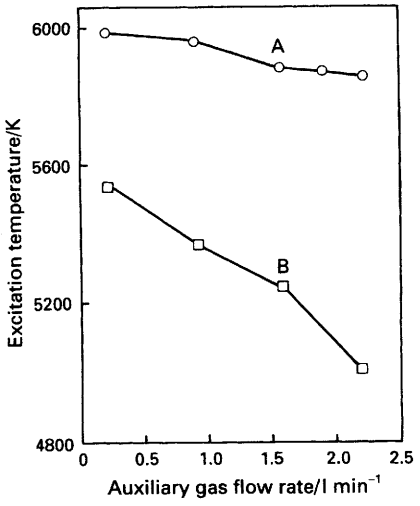

Fig. 10 Excitation temperature *versus* auxiliary gas flow rate: A, H_2O; and B, CCl_4. Observation height, 20 mm above load coil

The reduction of excitation temperature may be understood in terms of plasma energy transfer. When the total solvent loading is held constant, by keeping constant the plasma gas flow rate, nebulizer gas flow rate, liquid uptake rate and condenser temperature, *etc.*, the distribution of solvent loading in the plasma central channel may still be altered by changing the auxiliary gas flow rate. An increase in auxiliary gas flow rate carries more organic aerosol from the peripheral regions of the plasma into the plasma central channel. The presence of more C_2 species in the central channel, revealed by C_2 emission–height profiles, exerts a stronger interaction with the plasma. The dissociation of C_2 species therefore absorbs plasma energy that would otherwise have been available for the excitation process. As a result, the analyte intensity decreases, analyte emission–height profiles are shifted to a higher position and the ion-to-atom intensity ratios decrease. In this sense, C_2 emission intensity and its spatial behaviour may be used to evaluate the distribution of solvent loading in the plasma central channel. Based on the above discussion, it appears to be beneficial with organic sample introduction to achieve the highest excitation temperatures by not using an auxiliary gas. However, this is not feasible because of the practical limitation of carbon deposition on the plasma torch. Therefore, as a compromise condition, the lowest possible auxiliary gas flow rate is desirable so that good analytical performance can be obtained without significant carbon deposition. On the other hand, the effect of auxiliary gas flow rate on an aqueous plasma is negligible, for two main reasons: the bond dissociation energy of OH species is 4.3 eV, which is smaller than the dissociation energy of C_2 species of 6.5 eV, and the amount of aqueous solvent loading on the plasma is much smaller than with organic solvents, such as CCl_4.[14]

Conclusions

Several important conclusions may be drawn from this study. The plasma excitation conditions may be varied by the changing solvent distribution in the plasma with an auxiliary gas flow, even without a change in the total solvent loading reaching the plasma or in the nature of the solvent pyrolysis products. Further, the distribution of solvent loading in the plasma central channel plays a very important role in determining plasma conditions. For an organic plasma, an increase in auxiliary gas flow rate increases the level of C_2 species in the plasma channel. This in turn increases the solvent–plasma interaction, and more plasma energy is consumed by the dissociation of C_2 species. As a result, the excitation temperature decreases with increasing auxiliary gas flow rate and the analyte emission intensity decreases with increasing nebulizer gas flow rate.

The distribution of solvent aerosols in the plasma central channel may also be controlled with changes in the auxiliary gas flow rate. With aqueous solvents, however, the auxiliary gas flow rate has little effect on the plasma when an aqueous solvent is introduced.

Studies of emission–height profiles for C, C_2 and CN species indicate that these three species have different power response behaviours. Atomic C behaves like a hard line and C_2 acts as a soft line, whereas the CN species shows both hard line and soft line behaviour, depending on the location of CN species in the plasma.

Special attention should be given to the control of auxiliary gas flow rate when organic samples which give strong C_2 emission intensities are introduced. For optimum performance, the lowest possible auxiliary gas flow rate and a higher viewing height than with the corresponding aqueous solvent should be used. A higher forward r.f. power is also desirable to enhance decomposition of organic matrices at higher auxiliary gas flow rates.

This paper is based on work supported by the National Science Foundation under Grant No. CHE88-08183.

References

1 Caughlin, B. L., and Blades, M. W., *Spectrochim. Acta, Part B*, 1987, **42**, 353.
2 Murillo, M., and Mermet, J. M., *Spectrochim. Acta, Part B*, 1987, **42**, 1151.
3 Long, S. E., and Browner, R. F., *Spectrochim. Acta, Part B*, 1988, **43**, 1461.
4 Boorn, A. W., Cresser, M. S., and Browner, R. F., *Spectrochim. Acta, Part B*, 1980, **35**, 823.
5 Boorn, A. W., and Browner, R. F., *Anal. Chem.*, 1982, **54**, 1402.
6 Boumans, P. W. J. M., and Lux-Steiner, M. Ch., *Spectrochim. Acta, Part B*, 1982, **37**, 97.
7 Benli, H., *Spectrochim. Acta, Part B*, 1983, **38**, 81.
8 Maessen, F. J. M. J., Seeverens, P. J. H., and Kreuning, G., *Spectrochim. Acta, Part B*, 1984, **39**, 1171.
9 Blades, M. W., and Caughlin, B. L., *Spectrochim. Acta, Part B*, 1985, **40**, 79.
10 Olesik, J. W., and Den, S.-J., *Spectrochim. Acta, Part B*, 1990, **45**, 731.
11 Goldfarb, V. M., and Goldfarb, H. V., *Spectrochim. Acta, Part B*, 1985, **40**, 177.
12 Kreuning, G., and Maessen, F. J. M. J., *Spectrochim. Acta, Part B*, 1987, **42**, 677.
13 Kreuning, G., and Maessen, F. J. M. J., *Spectrochim. Acta, Part B*, 1989, **44**, 367.
14 Pan, C., Zhu, G., and Browner, R. F., *J. Anal. At. Spectrom.*, 1990, **5**, 537.
15 Fassel, V. A., Peterson, C. A., and Abercrombie, F. N., *Anal. Chem.*, 1979, **48**, 516.
16 Corliss, C. H., and Bozman, W. R., *Experimental Transition Probabilities for Spectral Lines of Seventy Elements (NBS Monograph*, No. 53), National Bureau of Standards, Washington, DC, 1962.
17 Barrett, P., and Pruszkowska, E., *Anal. Chem.*, 1984, **56**, 1927.
18 Boumans, P. W. J. M., *ICP Inf. Newsl.*, 1978, **4**, 89.
19 Edmonds, T. E., and Horlick, G., *Appl. Spectrosc.*, 1977, **31**, 536.
20 Kawaguchi, H., Ho, T., and Mizuike, A., *Spectrochim. Acta, Part B*, 1981, **36**, 615.
21 Long, S. E., and Browner, R. F., *Spectrochim. Acta, Part B*, 1986, **41**, 639.
22 Caughlin, B. L., and Blades, M. W., *Spectrochim. Acta, Part B*, 1985, **40**, 1539.

Paper 1/05739A
Received November 12, 1991
Accepted May 29, 1992